

DNA, RNA, and DNA/RNA Oligomer Duplexes: A Comparative Study of Their Stability, Heat, Hydration, and Mg^{2+} Binding Properties

Besik I. Kankia and Luis A. Marky*

Departments of Pharmaceutical Sciences, Biochemistry & Molecular Biology,
University of Nebraska Medical Center, 986025 Nebraska Medical Center, Omaha, Nebraska 68198-6025

Received: May 19, 1999

We used a combination of spectroscopic, calorimetric, density, and ultrasonic techniques to determine complete thermodynamic profiles, including hydration effects, for the formation of a set of DNA, RNA, and DNA/RNA oligomer duplexes, from the mixing of their complementary strands. UV melting curves show that at room temperature all four molecules are in the duplex state while the circular dichroism spectra indicate that the DNA duplex is in the “B” conformation and the RNA and DNA/RNA hybrid duplexes are in the “A” conformation. The favorable formation of these duplexes at 20 °C is characterized with exothermic enthalpies and unfavorable entropies, the RNA duplex is the more stable one, resulting from a more favorable heat of 7–17 kcal/mol. The volume and compressibility measurements show that the formation of each duplex is accompanied by an uptake of water molecules and that the overall hydration of a duplex is mainly determined by its conformation; the DNA duplex is 2-fold more hydrated than any of the other three duplexes. We also used density and ultrasonic techniques to determine the changes in the apparent molar volume, $\Delta\Phi V$, and adiabatic compressibility, $\Delta\Phi K_S$, for the interaction of Mg^{2+} with each duplex and its component single strands. These $\Delta\Phi V$ and $\Delta\Phi K_S$ values range from 2.2 cm^3/mol and $6.0 \times 10^{-4} \text{ cm}^3/(\text{mol bar})$ to 10.0 cm^3/mol and $21.9 \times 10^{-4} \text{ cm}^3/(\text{mol bar})$, respectively. The magnitude of the lowest values for the interaction of Mg^{2+} with the RNA duplex suggests the formation of Mg^{2+} –RNA outer-sphere complexes. However, the magnitude of the higher values for the interaction of Mg^{2+} with the DNA duplex, and two of the single strands, may be consistent with the formation of Mg^{2+} –nucleic acid inner-sphere complexes. Furthermore, the resulting $\Delta\Phi V/\Delta\Phi K_S$ ratios of $\sim 0.75 \times 10^4$ (formation of duplexes) and $\sim 0.48 \times 10^4$ (Mg^{2+} binding) suggest the uptake of mostly hydrophobic water and release of mostly electrostricted water, respectively.

Introduction

Water plays a fundamental role in the stability and overall secondary and tertiary structure of macromolecules.^{1,2} The physical and chemical properties of a nucleic acid molecule depend on the nucleotide sequence, conformation, ion binding, and overall hydration.¹ Experimental and theoretical investigations have indicated that nucleic acid double helices are heavily hydrated,^{1,3–7} for instance, X-ray and NMR investigations have shown that water molecules create an ordered structure, called “the spine of hydration”, in the minor groove of AT base pairs in the B conformation;^{8–12} water bridges are also found within adjacent phosphate groups of A- and Z-DNA.^{13–17} In solution, the overall hydration of a nucleic acid duplex depends on its conformation, nucleotide composition, and sequence.^{18–25} However, despite extensive investigations on the hydration of nucleic acids, the detailed nature of this phenomenon remains unknown. The main reason for this is the simultaneous presence of two distinctive types of hydrating water around a nucleic acid molecule: hydrophobic or structural (around nonpolar groups) and electrostricted (around polar and/or charged groups).^{26,27} These two types of water are difficult to detect and differentiate, complicating the measurement and analysis of their physical properties. Furthermore, the overall hydration of a nucleic acid molecule is closely associated with its number and type of condensed cations because these counterions are also hydrated.²⁸

A typical example is the interaction of divalent ions with nucleic acids: the close association of these metal ions involves the overlapping of their hydration shells, resulting in a release of water molecules,^{29,30} and the magnitude of the effect is determined by the actual position of the cation relative to the surface of DNA. For instance, a larger dehydration effect takes place in the formation of inner-sphere counterion–DNA complexes relative to the formation of outer-sphere complexes. For this reason, Mg^{2+} ions have been used to probe the overall hydration of nucleic acids using ultrasonic and density techniques.^{29,30}

In this work, we used a combination of spectroscopy, ultrasonic, and density techniques to investigate the energetics and hydration effects that accompany the formation of DNA, RNA, and DNA/RNA oligomer duplexes (see Figure 1). We also report on the hydration changes that take place on the interaction of Mg^{2+} with each duplex and their component single strands. Circular dichroism shows that the DNA oligomer duplex is in the B-like conformation while the RNA and DNA/RNA hybrid duplexes are in the A-like conformation. UV-melting curves indicate that the higher thermal stability of the RNA duplex, by 11–13 °C, over the DNA and hybrid duplexes, is primarily due to its higher favorable heat of formation. Direct ultrasonic and volumetric batch experiments show that duplex formation is accompanied by an uptake of structural water molecules. The overall hydration for the DNA duplex is roughly twice that for the RNA and DNA/RNA hybrid duplexes. The

* To whom correspondence should be address.

Single Strands:	Duplexes:
5'-d(CCATCGCTACC)-3' (ssDNA1)	5'-d(CCATCGCTACC)-3' 3'-d(GGTAGCGATGG)-5' (DNA)
5'-d(GGTAGCGATGG)-3' (ssDNA2)	5'-d(CCATCGCTACC)-3' 3'-r(GGUAGCGAUGG)-5' (HYB1)
5'-r(CCAUCGCUACC)-3' (ssRNA1)	5'-r(CCAUCGCUACC)-3' 3'-d(GGTAGCGATGG)-5' (HYB2)
5'-r(GGUAGCGAUGG)-3' (ssRNA2)	5'-r(CCAUCGCUACC)-3' 3'-r(GGUAGCGAUGG)-5' (RNA)

Figure 1. Sequences, and their designations, of single strands and duplexes used in this work.

interaction of Mg^{2+} with each duplex, or single strand, releases electrostricted water molecules. The overall thermodynamic data and hydration parameters are discussed in terms of duplex conformation, nucleotide sequence, type of hydrating water, and the formation of inner- and outer-sphere Mg^{2+} -nucleotide complexes.

Materials and Methods

Materials. All four oligonucleotides were synthesized by the Core Synthetic Facility of the Eppley Research Institute at UNMC, HPLC purified, and desalted by column chromatography. The oligonucleotides were further desalted by dialysis at 4 °C against water using Spectrum dialysis tubing with a molecular weight cutoff of 500 Da. The concentration of the oligomer solutions was determined at 260 nm and 80 °C using the following molar extinction coefficients, in $\text{mM}^{-1}\text{cm}^{-1}$ of strands: 98 for 5'-d(CCATCGCTACC)-3', 115 for 5'-d(GGTAGCGATGG)-3', 99 for 5'-r(CCAUCGCUACC)-3', and 118 for 5'-r(GGUAGCGAUGG)-3'. These values were calculated by extrapolation of the tabulated values of the dimers and monomer bases³¹ at 25 °C to high temperatures using procedures reported earlier.³² MgCl_2 , from Fisher, was used without further purification, and its water content was determined from ultrasonic velocity measurements of its aqueous solutions at 25 °C.³³ All measurements were performed in buffer solutions consisting of 10 mM Hepes, 100 mM NaCl, adjusted to pH 7.5.

Circular Dichroism (CD). Evaluation of the conformation of each duplex was obtained by simple inspection of their CD spectrum. The spectrum of each duplex at room temperature was obtained on a JASCO J-710 spectropolarimeter using a 0.5 mm quartz cell, which allows for the determination of the conformation of each duplex at the concentrations used in the ultrasonic and volumetric experiments.

Temperature-Dependent UV Spectroscopy. Absorbance versus temperature profiles (melting curves) for each duplex were measured at 260 nm with a thermoelectrically controlled Aviv 14-DS spectrophotometer and as a function of strand concentration. The temperature was scanned at a heating rate of 0.5 °C/min. These melting curves allow us to measure transition temperatures, T_M , which are the midpoint temperatures of the order-disorder transition of the duplexes, and van't Hoff enthalpies, ΔH_{vH} and ΔH_{CD} , using a two-state transition approximation as reported previously.³⁴

Ultrasonic Velocity Measurements. Relative ultrasonic velocity measurements were made with a home-built instrument,

based on the resonator method,³⁵ using a frequency range of 7–8 MHz. The influence of temperature fluctuations on these measurements was eliminated by using differentially two identical cells (reference and sample) of 0.7 mL each. Both cells were connected to a common circulating water bath, and their temperature difference was less than 0.2 mdeg. The molar increment of ultrasonic velocity, A , for a dilute solution is defined by the relationship $A = (U - U_0)/(U_0C)$, where U and U_0 are the ultrasonic velocities of the solution and solvent, respectively, and C is the solute concentration. The relative experimental error in the measurement of $(U - U_0)/(U_0)$ is $2 \times 10^{-5}\%$. The change in the molar increment of ultrasound velocity, ΔA , accompanying the formation of a duplex from the mixing of its complementary strands is given by the relationship: $\Delta A = (m_{12}U_{12} - m_1U_1 - m_2U_2)/(m_1U_0C_1)$, where m_1 , m_2 , and m_{12} are the masses of each component strand 1 and 2 and the mass of the duplex, respectively, U_1 , U_2 , and U_{12} are the ultrasound velocities of the solutions of each component strand 1 and 2 and that of the duplex, respectively, and C_1 is the molar concentration of component 1. All ΔA values were calculated in terms of the concentration of the limiting strand.

In the Mg^{2+} acoustical titrations, each single strand or duplex is titrated with Mg^{2+} , and 2–5 μL aliquots of MgCl_2 were added stepwise, using calibrated 10 μL Hamilton syringes, to a 695 μL oligomer solution in the sample cell. Mixing was performed directly in the sample cell with a built-in magnetic stirrer. The reference cell was filled with water and was left untouched during the course of each titration. Each of the resulting ultrasonic velocity values was corrected for the contribution of salt concentration, by carrying out similar titrations of the buffer; this allowed us to estimate the net effects of the interaction of Mg^{2+} with each oligonucleotide. The ΔA values are calculated with the equation $\Delta A = A - A_0$, where A is the molar increment of ultrasonic velocity of the oligomer and Mg^{2+} solution and A_0 is the molar increment of ultrasonic velocity of the free Mg^{2+} oligomer solution.

Density Measurements. The density of each oligomer (single strand or duplex) solution was measured with a DMA-602 densimeter (Anton Paar, Graz, Austria). As in the case of the acoustical measurements, a differential system consisting of two 0.2 mL cells was used. The apparent molar volume, ΦV , is calculated using the equation²⁸ $\Phi V = M/\rho - (\rho - \rho_0)/(\rho_0C)$, where ρ_0 and ρ are the density of the solvent and solution, respectively, and M is the molecular weight of the oligomer. The molar volume change, $\Delta\Phi V$, of duplex formation is calculated from the relationship $\Delta\Phi V = (m_1\rho_1 + m_2\rho_2 - m_{12}\rho_{12})/(m_1\rho_1C_1)$, where m and ρ correspond to the mass and density for each of the component single strands (1 or 2) and duplex (12). One of the strands is considered as the limiting reagent. To ensure the complete formation of duplexes, solutions of the 1:1 mixtures of complementary strands were heated to 50 °C and cooled to the measuring temperature of 20 °C. The $\Delta\Phi V$ accompanying the interaction of Mg^{2+} with each oligomer is calculated using the equation $\Delta\Phi V = \Phi V - \Phi V_0$, where ΦV is the apparent molar volume of the Mg^{2+} -oligomer solution and ΦV_0 is the apparent molar volume of the free oligonucleotide solution. In these experiments, the total effects are calculated per mole of phosphate, the strand or duplex is considered as the limiting reagent, and Mg^{2+} is in large excess. All solutions were prepared by weight using a microbalance, and extra precautions were taken to prevent evaporation of the weighted samples.

Determination of the Apparent Molar Adiabatic Compressibility. The change in the molar adiabatic compressibility,

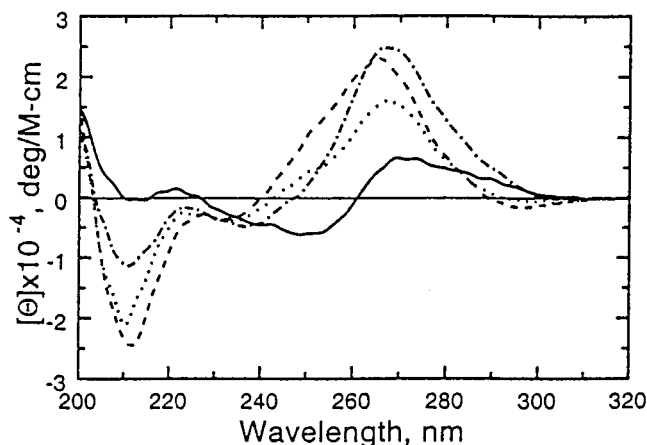


Figure 2. Circular dichroism spectra of the duplexes (~ 0.2 mM in strands) in 10 mM Hepes buffer, 100 mM NaCl, at pH 7.5 and 23 °C: DNA (solid line), RNA (dashed line), HYB-1 (dotted line), and HYB-2 (dotted-dashed line).

$\Delta\Phi K_S$, is determined from the changes in ΔA and $\Delta\Phi V$ according to the relationship³⁶ $\Delta\Phi K_S = 2\beta_0(\Delta\Phi V - \Delta A)$, where β_0 is the adiabatic compressibility coefficient of the solvent.

Hydration Contributions to the Apparent Volume and Apparent Adiabatic Compressibility Parameters. The molecular interpretation of the apparent molar volume, ΦV , and the apparent molar adiabatic compressibility, ΦK_S , are based on the following relationships:³⁷

$$\Phi V = V_m + \Delta V_h \quad \text{and} \quad \Phi K_S = K_m + \Delta K_h$$

The V_m term is the intrinsic molar volume of the solute molecule, while K_m is the intrinsic molar compressibility of this volume, which is inaccessible to the surrounding solvent. ΔV_h represents the actual hydration contribution that corresponds to the change in volume of the water around the solute molecule as a result of the solute–water interactions and the void volume between the solute molecule and that of the surrounding water. Similarly, ΔK_h is the hydration contribution to the apparent molar adiabatic compressibility, consisting of the changes in the compressibility of water around the solute molecule and the compressibility of the void volume between the solute molecules and of the surrounding water. The values of V_m and K_m for simple hydrophilic molecules and oligonucleotides, without significant inner cavities, are small relative to their hydration terms, ΔV_h and ΔK_h . Furthermore, the values of V_m and K_m remain constant in the absence of significant conformational changes and during the course of a titration of a duplex with Mg^{2+} . Therefore, the particular changes in the values of ΦV and ΦK_S are simply a reflection of their hydration changes: $\Delta\Phi V = \Delta\Delta V_h$ and $\Delta\Phi K_S = \Delta\Delta K_h$.

Results

CD Spectroscopy. The room temperature CD spectra for all duplexes are shown in Figure 2, the strand concentrations are similar to those used in acoustical measurements. The DNA duplex exhibits a CD spectra characteristic of a right-handed helix in the “B” conformation, whereas the spectra of the other three duplexes are characteristic of duplexes in the “A” conformation. The overlay of the spectra of the RNA and DNA/RNA hybrid duplexes shows an isoelliptic point at 231 nm. The positive bands present some differences in the magnitude and location of their maximum, which is consistent with the higher percentage of purine bases of one of the strands and/or the composition of the strands. For instance, the shift of the

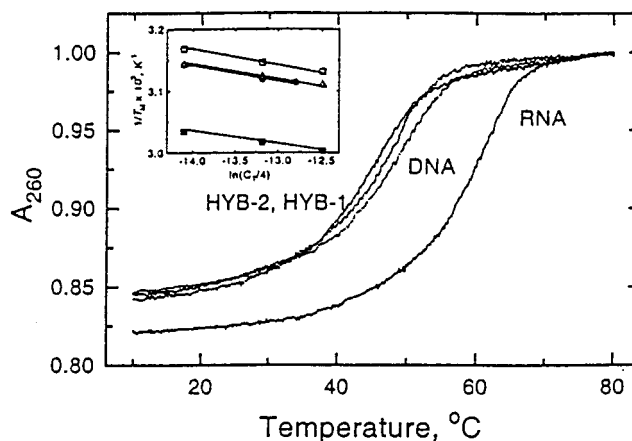


Figure 3. Normalized UV melting curves of the duplexes (~ 4 μ M in strands) in 10 mM Hepes buffer, 100 mM NaCl at pH 7.5. Inset: Dependence of T_M on strand concentration: DNA (closed circles), RNA (closed squares), HYB-1 (open triangles), and HYB-2 (open squares).

TABLE 1: Thermodynamic Parameters for the Helix–Coil Transition of Duplexes^a

duplex	T_M (°C)	ΔH_{shape} (kcal/mol)	ΔH_{ConDep} (kcal/mol)	ΔH_{pred} (kcal/mol)
DNA	55.3 (± 0.5)	82 (± 12)	86.3 (± 6)	85 (84)
RNA	65.8 (± 0.5)	91 (± 14)	103.4 (± 7)	114
HYB-1	54.2 (± 0.5)	90 (± 14)	95.7 (± 7)	99
HYB-2	52.4 (± 0.5)	89 (± 13)	86.9 (± 6)	90

^a All values determined in 10 mM Hepes, 100 mM NaCl, pH 7.5 at 20 °C. The T_M values refer to a total strand concentration of 15 μ M. ΔH_{ConDep} values are reported with an additional significant figure to allow for better accuracy in T_M and ΔG° calculations. ΔH_{pred} values have been estimated from the nearest-neighbor parameters of refs 41–43; the value in parentheses for the DNA duplex is from ref 44.

maximum to shorter wavelengths is due to the presence of uridine residues while their magnitude intensities are inversely proportional to the stability of the particular DNA/RNA hybrid.^{38,39} The CD spectrum of the HYB-1 duplex is between the RNA and DNA duplex spectra. We have not pursued any further analysis of these spectra, other than to show that the two hybrid duplexes have an A-like conformation.

Helix–Coil Transition of Duplexes. The UV melting curves of the 1:1 duplexes at 260 nm are shown in Figure 3. These curves show that at temperatures below 25 °C, all four molecules are in the duplex state, which allows us to choose 20 °C as our optimum experimental temperature for the volumetric and acoustical measurements. Above 25 °C all curves follow the characteristic sigmoidal behavior for the unfolding of a nucleic acid duplex. The thermal stability of these duplexes are in the following order: RNA \gg DNA > HYB-1 > HYB-2.

We used van't Hoff analysis to determine the unfolding enthalpies for the helix–coil transition of each duplex in two different ways: ΔH_{shape} from the shape of the melting curve and ΔH_{ConDep} from the dependence of T_M on strand concentration. The latter values are used for discussion in the following sections because they are determined more accurately; see Table 1. We measured endothermic heats for the unfolding of each duplex and these values, obtained from the slopes of the T_M – $\ln(C_T/4)$ curves, are in the order RNA > HYB-1 > HYB-2 \sim DNA; see inset of Figure 3 and Table 1. The overall ranking is in fair agreement with those obtained with similar sets of duplexes.^{38–40} Furthermore, the ΔH_{ConDep} values, determined in 0.1 M NaCl, are in excellent agreement with the enthalpy values calculated from DNA, RNA, and DNA/RNA nearest-neighbor parameters in 1 M NaCl.^{41–44} This comparison is

TABLE 2: Experimental Ultrasonic and Density Parameters for the Formation of Duplexes^a

duplex	ΔA (cm ³ /mol)	$\Delta\Phi V$ (cm ³ /mol)	$10^{-4}\Delta\Phi K_s$ [cm ³ /(mol bar)]
DNA	57.2	-133.1	-173.8
RNA	36.3	-74.8	-100.1
HYB-1	30.8	-73.7	-95.7
HYB-2	26.4	-71.5	-88.0

^a All values determined in 10 mM Hepes, 100 mM NaCl, pH 7.5 at 20 °C, and calculated per mole of duplex. The experimental uncertainties are as follows: ΔA (± 5), $\Delta\Phi V$ (± 8), $\Delta\Phi K_s$ ($\pm 13 \times 10^4$).

justified in this range of salt concentrations and is based on the small contribution of electrostatic interactions to the overall heat of unfolding.⁴⁵ The more stable RNA duplex unfolds with a higher endothermic heat of 17 kcal/mol while the DNA duplex has a higher T_M and lower enthalpy than the hybrid duplexes.

We used standard procedures³⁴ to determine the entropy for the helix-coil transition of each duplex from the intercepts of the T_M -concentration dependence plots. In this calculation, the enthalpy and entropy terms are assumed to be independent of temperature, i.e., $\Delta C_p = 0$, and have been found to be small for the formation or unfolding of a nucleic acid duplex.^{45,46} The Gibbs equation, $\Delta G = \Delta H - T\Delta S$, is used to calculate the corresponding free energy terms at 20 °C. The formation of each duplex at 20 °C is accompanied by favorable free energy terms resulting from the characteristic compensation of a favorable enthalpy and unfavorable entropy terms. In general, these favorable enthalpy terms correspond mainly to forming base-pair stacking interactions while the unfavorable entropy terms arise from contributions of the unfavorable association of two strands and uptake of both counterions and water molecules.

Hydration Parameters. In the following sections, the experimental data obtained from ultrasonic and density techniques will be presented in the order (a) formation of duplexes and (b) binding of Mg^{2+} to duplexes and single strands.

Ultrasonic Measurements. Table 2 lists the changes in the increments of ultrasound velocity that accompany the formation of a duplex from the mixing of its complementary strands. All values are positive and show that the formation of each duplex is accompanied by an uptake of water molecules; this is consistent with the formation of base-pair stacks in a double helical structure with a larger charge density parameter. The magnitude of these ΔA values are in the following order DNA \gg RNA $>$ HYB-1 $>$ HYB-2, the higher ΔA value for the formation of the DNA duplex clearly indicates a higher uptake of water molecules by this molecule. To a first approximation this is consistent with previous results of the B-like conformation as being the one with a higher hydration level.^{18,22,23}

Acoustical titrations for the addition of Mg^{2+} to each of the four duplexes are shown in Figure 4; these curves can be considered as Mg^{2+} binding isotherms, and their shapes are similar, resembling exponential decay curves. However, fundamental differences are seen in the initial slopes and overall amplitude of the curves. The initial slopes are proportional to the Mg^{2+} -nucleic acid duplex binding affinities ($K_{Mg^{2+}}$), while the overall amplitude at $[Mg^{2+}]/[phosphate]$ saturation levels of ~ 6 correspond to the total dehydration effect of Mg^{2+} binding, $\Delta A_{Mg^{2+}}$; see Figure 4. The interaction of Mg^{2+} with each duplex yielded negative values of $\Delta A_{Mg^{2+}}$, which are consistent with a release of water molecules. This water release corresponds to the net hydration changes of the exchange of Na^+ for Mg^{2+} in the ionic atmosphere of the counterion-nucleic acid complex. The hydration contribution of Na^+ is considered

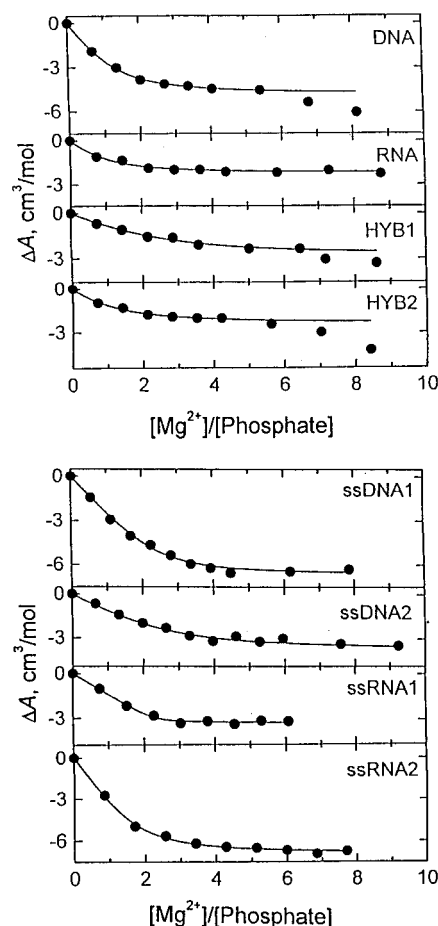


Figure 4. Ultrasonic titration curves of the single strands (top panel) and duplexes (bottom panel) with $MgCl_2$ in 10 mM Hepes buffer, 100 mM NaCl, at pH 7.5 and 20 °C. The initial concentration of strand or duplex is ~ 2.2 mM in phosphate; the total dilution effect was less than 10%. The measured ΔA values are given per phosphate, and the solid lines correspond to the three-parameter nonlinear fits of the experimental points up to $[Mg^{2+}]/[phosphate]$ ratios of 6.

negligible. A quantitative evaluation of both $K_{Mg^{2+}}$ and $\Delta A_{Mg^{2+}}$ is determined from fitting the Mg^{2+} -binding isotherms interactively, as described previously.²⁹ This fitting procedure is based on the binding model where Mg^{2+} interacts with the nucleic acid lattice containing one type of identical and independent binding sites, which are characterized by three parameters: $K_{Mg^{2+}}$, $\Delta A_{Mg^{2+}}$, and the apparent number of Mg^{2+} counterions per binding site, $n_{Mg^{2+}}$. To simplify this fitting procedure, the $n_{Mg^{2+}}$ value was assumed constant and equal to 0.5; i.e., one Mg^{2+} interacts with two negatively charged phosphate groups, as was done earlier.²⁹ We obtained $\Delta A_{Mg^{2+}}$ values, per mole of Mg^{2+} , ranging from -4.4 to -10.0 cm³/mol (Table 3) and $K_{Mg^{2+}}$ values ranging from 180 to 780 M⁻¹ (data not shown). The strength of Mg^{2+} binding to the duplexes is in the order RNA $>$ DNA \sim HYB-2 $>$ HYB-1, but a higher release of water molecules is obtained with the DNA duplex. Furthermore, with the exception of Mg^{2+} -RNA, the other three ultrasonic curves show ΔA values decreasing at higher $[Mg^{2+}]/[phosphate]$ ratios, which may be the result of additional binding sites yielding conformational changes and/or aggregation of these duplexes.

The Mg^{2+} -single strands acoustical titrations are shown in Figure 4. Mg^{2+} binding yielded $\Delta A_{Mg^{2+}}$ values in the range of -6.5 to -14 cm³/mol (see Table 3) consistent with the release of water molecules. The $K_{Mg^{2+}}$ values are in the order ssRNA2 $>$ ssRNA1 $>$ ssDNA1 \sim ssDNA2 and range from 240 to 380

TABLE 3: Experimental Ultrasonic and Density Parameters for the Interaction of Mg^{2+} Ions with Duplexes and Their Component Single Strands^a

duplex or single strand	$\Delta A_{\text{Mg}^{2+}}$ (cm^3/mol)	$\Delta \Phi V$ (cm^3/mol)	$10^{-4} \Delta \Phi K_S$ [$\text{cm}^3/(\text{mol bar})$]
DNA	-10.0	6.0	14.6
RNA	-4.4	2.2	6.0
HYB-1	-6.0	2.6	7.8
HYB-2	-5.0	4.2	8.4
ssDNA1	-13.4	9.8	21.4
ssDNA2	-7.4	4.8	11.1
ssRNA1	-6.5	4.8	10.3
ssRNA2	-14.0	10.0	21.9

^a All values determined in 10 mM Hepes, 100 mM NaCl, pH 7.5 at 20 °C. These values are calculated per mole of base pairs and also correspond to the interaction of Mg^{2+} with two phosphate groups. The experimental uncertainties are as follows: ΔA (± 1), $\Delta \Phi V$ (± 1.5), $\Delta \Phi K_S$ ($\pm 2.5 \times 10^4$).

M^{-1} (data not shown). All curves do not show a further decrease of ΔA values at high $[\text{Mg}^{2+}]/[\text{phosphate}]$ ratios.

The comparison of the Mg^{2+} binding to duplexes and single strands reveals that the binding is somewhat stronger with the duplexes by an average factor of 1.7, which is consistent with the higher charge density parameter of the duplexes. On the other hand, the dehydration effects are stronger with the single strands by an average factor of 1.5, which may be due to a greater exposure of organic groups to the solvent, yielding an increased participation of structural water.

Volume and Compressibility Effects. The changes of the apparent molar volume, and the derived apparent molar adiabatic compressibility accompanying the formation of each duplex, are listed in Table 2. The negative signs of these two parameters also indicate that duplex formation is accompanied by an uptake of water molecules. This uptake is very similar for all three duplexes in the "A" conformation, and the actual differences may reflect small changes in the hydration state among the single strands, prior to forming a particular duplex. The values of each parameter for the DNA duplex are a factor of 1.8 higher than the average value of the other three duplexes. The volume effect for the DNA duplex is in excellent agreement with earlier measurements with a magnetic suspension densimeter of the volume change of $-144 \text{ cm}^3/\text{mol}$.⁴⁷ Therefore, the results indicate that the uptake of water molecules in duplex formation is strongly dependent on the nucleic acid conformation.

The changes in the apparent molar volume and adiabatic compressibility for the binding of Mg^{2+} to the single strands and duplexes are shown in Table 3. All values are positive and consistent with the reported effects derived from the values of ΔA . Mg^{2+} binding is accompanied by a release of water molecules from the hydration shells of the free Mg^{2+} ions and/or interacting nucleic acid atomic groups. However, the interaction of Mg^{2+} with single strands yielded on the average higher $\Delta \Phi V$ and $\Delta \Phi K_S$ values that correspond to a 2-fold increase in the amount of water release. Among the pair of RNA single strands, a higher dehydration effect is observed with the strand with higher purine content while for the pair of DNA strands, a higher dehydration effect is observed with the strand with a higher pyrimidine content. In general, our results are in good agreement with earlier investigations on the interaction of cations with single strands and duplexes.^{29,30,48}

Discussion

The overall thermodynamic effects will be discussed in two sections: (i) formation of duplexes from the mixing of its two

TABLE 4: Complete Thermodynamic Profiles for the Formation of Duplexes at 20 °C^a

duplex	ΔG° (kcal/mol)	ΔH (kcal/mol)	$T\Delta S$ (kcal/mol)	ΔV (cm^3/mol)	$10^{-4} \Delta \Phi K_S$ [$\text{cm}^3/(\text{mol bar})$]
DNA	-9.3	-86.3	-77.0	-133	-174
RNA	-14.0	-103.4	-89.4	-75	-100
HYB-1	-10.0	-95.7	-85.7	-74	-96
HYB-2	-8.6	-86.9	-78.0	-72	-88

^a All values determined in 10 mM Hepes, 100 mM NaCl, pH 7.5 at 20 °C, and calculated per mole of duplex. ΔH and $T\Delta S$ values are reported with an additional significant figure to allow for better accuracy in T_M and ΔG° calculations. The experimental uncertainties are proportional to the ones reported in the previous tables.

complementary strands and (ii) the interaction of Mg^{2+} with single strands and duplexes.

Thermodynamics of Forming DNA, RNA, and DNA/RNA Duplexes. We have investigated four undecamer duplexes with similar sequences: one DNA, one RNA, and two hybrid DNA/RNA duplexes. Complete thermodynamic profiles for the formation of each duplex at 20 °C are listed in Table 4. For a better understanding of these profiles, we should emphasize the importance of taking into account contributions from the conformation, physical, and chemical properties of all participating species. These contributions include (i) base stacking interactions, hydration, and ion binding from the single and complementary strands and (ii) base-pairing and base-pair stacking of the particular duplex conformation, as well as its overall hydration and counterion binding. These noncovalent interactions depend on the actual chemical composition of the strands used. The formation of each duplex is accompanied by favorable free energy terms, enthalpy-entropy compensations, uptake of ions, and immobilization of water molecules; see Table 4. The observed exothermic enthalpies are the net balance of many contributions: base-pairing and base-pair stacking interactions of duplexes, disruption of base stacking interactions of single strands, uptake of water molecules by duplexes, and release of hydrophobic water from the single strands prior to going into the duplex state. The uptake of counterions has a negligible heat contribution.⁴⁹ The unfavorable entropy terms correspond to the contributions of a higher ordered system resulting from the bimolecular association of two strands and the net uptake of water and counterions by the duplex.

In this particular set of duplexes, the RNA duplex has the highest T_M and forms most favorably at 20 °C (Table 1) with the highest enthalpy term. The favorable free energy terms of this set roughly parallel in magnitude with the favorable enthalpy terms in the following order: RNA > HYB-1 > DNA ~ HYB-2 (Table 4). The thermodynamic profiles for the DNA duplex are in excellent agreement with a previous investigation.⁴⁷ For instance, in this investigation duplex formation yielded enthalpies of -82 and -80 kcal/mol obtained directly by isothermal titration calorimetry at 20 °C and differential scanning calorimetry, respectively, and in agreement with the value of -86 kcal/mol reported here. This indicates a negligible contribution of base-base stacking interactions of the DNA single strands and allows us to assume that base-base stacking of the RNA strands will contribute similarly in the formation of the RNA and hybrid duplexes. In general, contributions of stacking interactions are highly dependent on the base sequence and RNA single strand stacking interactions may be different than those in DNA strands. However, the above assumption may be valid with this set of duplexes because the pairs of DNA and RNA strands have equivalent base sequences and each strand has a symmetric sequence around the base at the center; see Figure 1. Furthermore, the main difference between the pairs of strands,

DNA vs RNA, is the pyrimidine substitution of two dT for two rU, and it is well-known that these bases have the lowest tendency to self-associate.⁵⁰ The contribution from base-pairing interactions is expected to be also similar among the four duplexes. An overall counterion uptake of 2.9 mol of Na⁺/mol of duplex has been measured for this DNA duplex,⁴⁷ and similar counterion uptake is expected in the formation of the other three duplexes, as has been the case for a similar set of homopurine/homopyrimidine polymer duplexes.¹⁸ Therefore, the observed heat differences of duplex formation may be due to a first approximation to differences in base-pair stacking and to changes in the overall hydration states of the single strands and duplex conformation.

Are the observed hydration changes contributing to the measured enthalpies of duplex formation? To answer this question, we should first discuss the hydration events that take place in the formation of a duplex from mixing two complementary strands. We have shown that the formation of each duplex is accompanied by negative values of ΦV and ΦK_S , which indicate that the duplex state has a higher degree of hydration than the two combined strands. Physically, a finite value of the volume change is obtained because of differences in the magnitude of the molar volume between hydrating water and bulk water (up to 6 mL/mol of water).^{26,27} The molar volume of water in the hydration shells of a nucleic acid also depends on the type of hydrating water; this could be structural (or hydrophobic) around organic moieties and nonpolar atomic groups or electrostricted around charges and polar atomic groups. In forming a nucleic acid duplex, additional contributions should be taken into consideration. These include the dehydration effects resulting from the association of two solute molecules, the pairing of nucleotide bases, stacking of base pairs, and the increased hydration of the duplex state (relative to the single strands) and due to its increased charged density parameter. Other hydration changes related to the interaction of univalent counterions with nucleic acid duplexes can be considered negligible because these bound counterions keep their hydration shells intact.⁵¹ The overall uptake of water molecules in the formation of a duplex is supported by density investigations of double-helical DNA.^{18,25,47} Other investigations have shown that the "B" conformation is the more hydrated one^{18,22,23} and that the formation of dA·dT base pairs are more hydrated than dG·dC base pairs.^{20,29} In this set of four duplexes, and relative to the duplexes in the "A" conformation, the formation of the DNA duplex is accompanied by almost a 2-fold higher hydration level, in agreement with earlier results of the hydration properties of DNA crystals^{8,9,13,17} and solution studies as a function of conformation.^{18,22,23} However, the reported values correspond to the hydration differences of a given duplex relative to its complementary strands, so one needs to take into account the chemical differences of the strands: the -OH groups of the RNA strands and the extra -CH₃ thymine groups of the DNA strands. These groups are hydrated and may increase the overall hydration of a particular single strand, thus lowering the relative hydration of the duplexes. On the other hand, the hydration parameters ($\Delta\Phi V$ and $\Delta\Phi K_S$ values) for the formation of the RNA and DNA/RNA hybrid duplexes are similar within experimental uncertainties. This result shows that the magnitude of the uptake of water molecules by a helical structure is determined mostly by its conformation and not by its chemical composition. Furthermore, duplexes with similar hydration (RNA and DNA/RNA hybrids) are characterized with slightly different enthalpies of formation. This may indicate that the reported hydration changes have a negligible contribution to

the measured enthalpy values unless the heat of removing structural water molecules from the single strands is compensated (or with opposite sign) by the heat of binding electrostricted water to the duplexes. For instance, the energy contribution of the hydration changes may be estimated from the $p\Delta V$ term; we obtained a value of 2.4 cal/mol of duplex using a $\Delta V = 100$ mL/mol of duplex at 1 atm pressure. This is a lower estimate, and in principle this energetic contribution is much higher because the immobilized water molecules around the charges of a duplex structure are experiencing an effective pressure in excess of 1000 atm but is still a small fraction of the observed differential heats of duplex formation. Therefore, hydration has a small contribution to the overall heats of duplex formation and most likely these water molecules have an important role in maintaining the particular structure and conformation of a nucleic acid duplex.

Hydration Effects in the Binding of Mg²⁺ to Single Strands and Duplexes. The interaction of Mg²⁺ with a nucleic acid has been considered to be electrostatic;^{52,53} this is consistent with the magnitude of the $K_{Mg^{2+}}$ reported here. However, to interpret the hydration effects that take place in the interaction of Mg²⁺ with single strands and duplexes, we have to consider how Mg²⁺ interacts with each type of molecule. Therefore, it is important to take into account the effective charge density and conformation of the nucleic acid molecule, its overall hydration level, and the inclusion of specific effects in terms of the formation of inner-sphere complexes, if any, when Mg²⁺ is chelating specific atomic groups of the oligonucleotide. Does Mg²⁺ interact directly with atomic groups of the oligonucleotides? Our $\Delta\Phi V$ and $\Delta\Phi K_S$ values of Mg²⁺ binding should be compared to similar parameters for complex formation or dissociation processes of metal ions with charged molecules of known three-dimensional structures. There are two useful reactions: the formation of Mg-EDTA complexes⁵⁴ and the dissociation of chloride ions from the *trans*- and *cis*-diammine-platinum.⁵⁵ In the Mg-EDTA²⁻ complex, Mg²⁺ makes six coordination bonds with four negatively charged oxygen and two polar nitrogen atoms, each of these coordinated bonds is characterized by a compressibility and volume effect of 22×10^{-4} cm³/(mol bar) and 8 cm³/mol, respectively.⁵⁴ The dissociation of one chloride ion from the *trans*- or *cis*-[Pt(NH₃)₂-Cl₂] complexes yields compressibility and volume effects of -18×10^{-4} cm³/(mol bar) and -5 cm³/mol, respectively, these values correspond to an increased hydration of the dissociated atoms. On the basis of these data, one can assume that the formation of one direct contact between Mg²⁺ and a polar or charged atomic group of a nucleic acid corresponds to a change in the volume and compressibility parameters of 5–8 cm³/mol and $(18-22) \times 10^{-4}$ cm³/(mol bar), respectively.

The positive $\Delta\Phi V$ and $\Delta\Phi K_S$ values of Mg²⁺ binding to each strand or duplex indicate a release of water molecules from the hydration shells of the participating atomic groups, the latter also correlates with the overall uptake of water molecules in the formation of each duplex; see Figure 5. The dehydration parameters of Table 4, reported per mole of base pair, indicate that the interaction of Mg²⁺ with ssDNA1, ssRNA2, and DNA are very close to the dehydration effects for the formation of inner-sphere complexes with one coordination bond. The dehydration effects for Mg²⁺ binding to other strands and duplexes are around half of the effect for one direct contact and suggest that their association takes place through the formation of outer-sphere complexes. Furthermore, the above estimations are also supported by the measurements of Millero and co-workers,⁵⁶ who reported ΔA values of -5 and -35 cm³

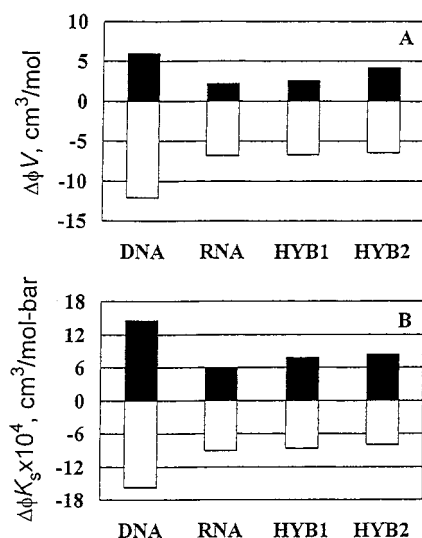


Figure 5. Panel A: Correlation of the $\Delta\Phi V$ values of duplex formation (filled rectangles) with those of Mg^{2+} binding to duplexes (open rectangles). Panel B: Correlation of the $\Delta\Phi K_s$ values of duplex formation (filled rectangles) with those of Mg^{2+} binding to duplexes (open rectangles). For a proper comparison, all values are given per base pairs. Both parameters indicate that the extent of increased hydration (positive values) in the formation of a duplex is proportional to the extent of the dehydration effects (negative values) of Mg^{2+} binding to the same duplex.

mol^{-1} for the formation of MgSO_4 and CaSO_4 complexes, respectively, and concluded that Mg^{2+} forms outer-sphere complexes while Ca^{2+} is forming inner-sphere complexes with SO_4^{2-} . The latter value corresponds to the coordination of three bonds between the interacting ions and the exclusion of ca. seven water molecules from the hydration shells of Ca^{2+} and SO_4^{2-} . Furthermore, Skerjanc and Strauss⁵⁷ using dilatometric measurements reported a ΔV of 6.4–8.7 cm^3/mol of Mg^{2+} in 0.2 M TMACl for the binding of Mg^{2+} to DNA, which also supports the formation of Mg –DNA inner-sphere complexes with just one coordination bond. It is also possible that the data could be interpreted as indicating a small fraction of contact ion pairs rather than all ion pairs are contact pairs. Alternatively, a more realistic picture of the hydration of charged ions and ionized polymer groups is that the inner layer is surrounded by a region that is fairly extensively electrostricted. And, the main contribution to the volume change of ion pairing is from the relaxation of the outer electrostricted region, with the removal of contact waters giving only a relatively small contribution to the volume. Therefore, the values of the volume changes reported here are probably not indicative of a singly coordinated inner-sphere contact complex, but instead support the idea that Mg^{2+} binding to all molecules relaxes only slightly the electrostricted region lying beyond the inner layers.

The formation of Mg –DNA inner-sphere complexes may be due to both its “B” conformation, which renders it more hydrated, and its 64% content of dG•dC base pairs that favors the formation of inner-sphere complexes.²⁹ The interaction of Mg^{2+} with the single strands yields higher $\Delta\Phi V$ and $\Delta\Phi K_s$ values, which indicates on the average, and relative to the duplexes, a 2-fold increase in the amount of water release. This may be explained in terms of a greater exposure of atomic groups to the solvent by the single strands. However, among the pairs of DNA or RNA single strands, the dehydration effect is nearly 2-fold higher with the DNA strand containing a higher percentage of pyrimidine bases and with the RNA strand containing a higher purine content; see Table 3. To explain these differences, we have to look at the chemical differences of the

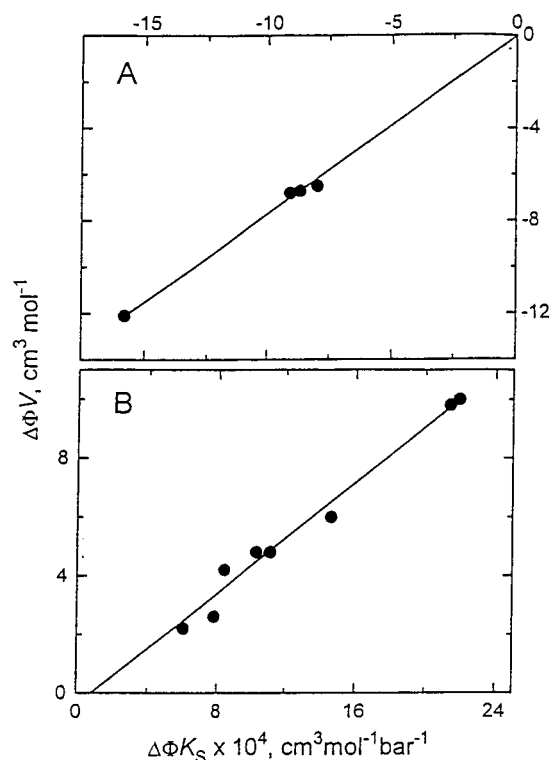


Figure 6. $\Delta\Phi V$ vs $\Delta\Phi K_s$ plots for duplex formation (panel A) and Mg^{2+} binding to oligonucleotides (panel B) in 10 mM Hepes buffer, 100 mM NaCl, at pH 7.5 and 20 °C. The $\Delta\Phi V$ and $\Delta\Phi K_s$ values are calculated per base pairs; the $\Delta\Phi V/\Delta\Phi K_s$ ratio or the slope of each plot might indicate the type of water, hydrophobic or electrostricted, involved in these processes.

strands; RNA strands have an additional OH group, which potentially could interact with Mg^{2+} . In addition, it is reasonable to think that single strands with higher purine content will have a higher degree of base–base stacking interactions, and also if we assume that similar degrees of stacking interactions take place among the strands with similar sequences, i.e., deoxy vs ribo. Then, the observed dehydration effects may be explained in terms of both the specific single strand conformation and the degree of exposure of nucleic acid atomic groups that are able to complex Mg^{2+} ions. A similar trend was found in our earlier work on the hydration parameters for the interaction of Mg^{2+} and Mn^{2+} with poly(rA) and poly(rU).⁴⁸ The poly(rA) strand, which is characterized with a well-defined single strand helical structure, showed higher dehydration effects in its interaction with these ions while the poly(rU) strand with a random coil conformation showed lower dehydration effects.

Types of Water Involved in Duplex Formation and Mg^{2+} Binding. The type of hydrating water, structural or electrostricted, responsible for the hydration effects in the processes of duplex formation and Mg^{2+} binding may be characterized by the absolute value of the ratio of $\Delta\Phi V/\Delta\Phi K_s$,^{54,58,59} defined as k , or by the slope of a plot of $\Delta\Phi V$ vs $\Delta\Phi K_s$ for a given type of process. Highly charged molecules, EDTA^{4-} and ions, are characterized by k values ranging from 0.34×10^4 to $0.39 \times 10^4 \text{ bar}$,⁵⁴ while the molecules with increasing nonpolar character have higher k values. For instance, the k values for the nucleic acid bases are $\sim 0.75 \times 10^4 \text{ bar}$.⁵⁹ The plots of $\Delta\Phi V$ vs $\Delta\Phi K_s$ yield nearly linear correlations for each type of process reported here (see Figure 6); we obtained slopes of 0.75×10^4 and $0.48 \times 10^4 \text{ bar}$ for the formation of duplexes and Mg^{2+} binding, respectively. These slope values indicate that the type of water involved in the formation of duplexes is primarily structural

water while the interaction of Mg^{2+} involves primarily electrostricted water. This means that the overall uptake of water molecules in the formation of each duplex results from the balance of several contributions. This includes the removal of structural water from the single strands, the net removal and immobilization of electrostricted water by polar and charged groups of the single strand and duplex, respectively, and immobilization of structural water by the grooves of the duplex. On the other hand, the release of water molecules on the binding of Mg^{2+} to oligonucleotides is the result of removing water molecules from polar and charged groups of the nucleic acid and from the Mg^{2+} ions.

Number of Water Molecules Involved in the Interaction of Mg^{2+} with Oligonucleotides. To estimate the number of water molecules, N , involved in the interaction of Mg^{2+} with a nucleic acid molecule, we assume that the amount of water released is purely electrostricted. We use the reported $\Delta\Phi V$ and $\Delta\Phi K_S$ values of Table 4 and the following equations:³⁷ $N = \Delta\Phi V / (V_h - V_w)$ and $N = \Delta\Phi K_S / (K_h - K_w)$, where V_h and K_h are the volume and compressibility of a water molecule released by the hydration shells and V_w and K_w are the volume and compressibility of bulk water, equal to 18 cm³/mol and 8.2×10^{-4} cm³/(mol bar), respectively. The change of the molar volume of water transferred from the hydration shell of an ion (or a nucleotide phosphate group) to bulk water, $V_w - V_h$, has been estimated to be equal to 2.5 mL/mol.^{56,60} These calculations yield a release of one water molecule per base pair for the binding of Mg^{2+} to RNA, HYB-1, HYB-2, ssDNA2, and ssRNA1, two water molecules from the DNA duplex, and three water molecules from the ssDNA1 and ssRNA2 strands. Similar values are obtained from the compressibility data using the assumption that water molecules are incompressible in their hydration shells.

To do the same estimation for the number of water molecules involved in the formation of a duplex is difficult because the resulting hydration changes of duplex formation involved a much higher percentage of structural water, for which we still do not know its apparent molar volume.

Conclusion

We have reported complete thermodynamic profiles and hydration parameters for the formation of a set of DNA, RNA, and DNA/RNA hybrid duplexes with equivalent sequences and have determined hydration parameters for the interaction of Mg^{2+} with each duplex and its component single strands. The DNA duplex is in the "B" conformation, while the RNA and the DNA/RNA hybrid duplexes are in the "A" conformation. The volume and compressibility measurements show that the formation of each duplex is mostly accompanied by the uptake of structural water molecules and that the overall hydration of a duplex is mainly determined by its conformation. The DNA duplex is the more hydrated one, while the more stable RNA duplex has the lowest hydration level. This allows us to speculate on the correlation of the hydration level with duplex flexibility; a duplex will have a more rigid conformation if it has a lower amount of structurally hydrating water. In addition, the resulting improved base-pairing and base-stacking interactions of a rigid conformation may be due to a reduced competition of water molecules for nucleic acid hydrogen bonding. The interaction of Mg^{2+} with each duplex and each of its component single strands is accompanied by a release of mostly electrostricted water; this correlates with the uptake of water molecules in the formation of duplexes. The lowest values of the hydration parameters were obtained with Mg^{2+} -RNA, which indicate the

formation of Mg^{2+} -RNA outer-sphere complexes. The higher $\Delta\Phi V$ and $\Delta\Phi K_S$ values for the interaction of Mg^{2+} -DNA, and two of the single strands, may be consistent with the formation of Mg^{2+} -nucleic acid inner-sphere complexes. These results will serve as thermodynamic baselines for the investigation of the interaction of Mg^{2+} with complex RNA molecules, in which Mg^{2+} plays a stabilizing role of the structure and conformation of these molecules.

Acknowledgment. This work was supported by Grant GM42223 from the National Institutes of Health.

References and Notes

- (1) Saenger, W. In *Principles of Nucleic Acid Structure*; Kantor, G. R., Ed.; Springer-Verlag: New York, 1984.
- (2) Tanford, C. *Adv. Protein Chem.* **1968**, *23*, 121.
- (3) Texter, J. *Prog. Biophys. Mol. Biol.* **1978**, *33*, 83.
- (4) Westhof, E. *Annu. Rev. Phys. Chem.* **1988**, *17*, 125.
- (5) Berman, H. M. *Curr. Opin. Struct. Biol.* **1991**, *1*, 423.
- (6) Tunis, M.-J. B.; Hearst, J. E. *Biopolymers* **1968**, *6*, 1325.
- (7) Garcia, A. E.; Hummer, G.; Soumpasis, D. M. In *Neutrons in Biology*; Schoenborn, B. P., Knott, R., Eds.; Plenum Press: New York, 1996; pp 299-308.
- (8) Drew, H. R.; Dickerson, R. E. *J. Mol. Biol.* **1981**, *151*, 535.
- (9) Kopka, M. L.; Fratini, A. V.; Drew, H. R.; Dickerson, R. E. *J. Mol. Biol.* **1981**, *163*, 129.
- (10) Alexeev, D. G.; Lipanov, A. A.; Skuratovskii, I. Ya. *Nature* **1987**, *325*, 821.
- (11) Kubinec, M. G.; Wemmer, D. E. *J. Am. Chem. Soc.* **1992**, *114*, 8739.
- (12) Shui, X.; McFail-Isom, L.; Hu, G. G.; Williams, L. D. *Biochemistry* **1998**, *37*, 8341.
- (13) Wang, A. H.-J.; Fujii, S.; van Boom, J. H.; Rich, A. *Proc. Natl. Acad. Sci. U.S.A.* **1982**, *79*, 3968.
- (14) Wang, A. H.-J.; Hakoshima, T.; van der Marel, G.; van Boom, J. H.; Rich, A. *Cell* **1984**, *37*, 321.
- (15) Westhof, E.; Prange, T.; Chevrier, B.; Moras, D. *Biochimie* **1985**, *67*, 811.
- (16) Chevrier, B.; Dock, A. C.; Hartmann, B.; Leng, M.; Moras, D.; Thuong, M. T.; Westhof, E. *J. Mol. Biol.* **1986**, *188*, 707.
- (17) Saenger, W.; Hunter, W. N.; Kennard, O. *Nature* **1986**, *324*, 385.
- (18) Rentzeperis, D.; Kupke, D. W.; Marky, L. A. *Biopolymers* **1993**, *33*, 117.
- (19) Mrevlishvili, G. M. *Dokl. Akad. Nauk SSSR* **1981**, *260*, 761.
- (20) Buckin, V. A.; Kankiya, B. I.; Bulichov, N. V.; Lebedev, A. V.; Gukovsky, V. P.; Sarvazy, A. P.; Williams, A. R. *Nature* **1989**, *340*, 321.
- (21) Macgregor, R. B., Jr.; Chen, M. Y. *Biopolymers* **1990**, *29*, 1069.
- (22) Buckin, V. A.; Kankiya, B. I.; Sarvazy, A. P.; Uedaira, H. *Nucl. Acids Res.* **1989**, *17*, 4189.
- (23) Umehara, T.; Kuwabara, S.; Mashimo, S.; Yagihara, S. *Biopolymers* **1990**, *29*, 649.
- (24) Preisler, R. S.; Chen, H. H.; Colombo, M. F.; Choe, Y.; Short, B. J., Jr.; Rau, D. C. *Biochemistry* **1995**, *34*, 14400.
- (25) Rentzeperis, D.; Kupke, D. W.; Marky, L. A. *Biochemistry* **1994**, *33*, 9588.
- (26) Frank, H. S.; Evans, M. W. *J. Chem. Phys.* **1945**, *13*, 507.
- (27) Kauzmann, W. *Adv. Protein Chem.* **1959**, *14*, 1.
- (28) Millero, F. J. In *Water and Aqueous Solutions*; Horn, R. A., Ed.; Wiley-Interscience: New York, 1972; pp 519-595.
- (29) Buckin, V. A.; Kankiya, B. I.; Rentzeperis, D.; Marky, L. A. *J. Am. Chem. Soc.* **1994**, *116*, 9423.
- (30) Buckin, V. A.; Tran, H.; Morozov, V.; Marky, L. A. *J. Am. Chem. Soc.* **1996**, *118*, 7033.
- (31) Cantor, C. R.; Warshaw, M. M.; Shapiro, H. *Biopolymers* **1970**, *9*, 1059.
- (32) Marky, L. A.; Blumenfeld, K. S.; Kozlowski, S.; Breslauer, K. J. *Biopolymers* **1983**, *22*, 1247.
- (33) Millero, F. J.; Ward, G. K.; Chetirkin, P. V. *J. Acoust. Soc. Am.* **1977**, *61*, 1492.
- (34) Marky, L. A.; Breslauer, K. J. *Biopolymers* **1987**, *26*, 1601.
- (35) Eggers, F.; Funck, T. *Rev. Sci. Instrum.* **1973**, *44*, 969.
- (36) Barnartt, S. *J. Chem. Phys.* **1952**, *20*, 278.
- (37) Shio, H.; Ogawa, T.; Yoshihashi, H. *J. Am. Chem. Soc.* **1955**, *77*, 4980.
- (38) Roberts, R. W.; Crothers, D. M. *Science* **1992**, *258*, 1463.
- (39) Ratmeyer, L.; Vinayak, R.; Zhong, Y. Y.; Zon, G.; Wilson, W. D. *Biochemistry* **1994**, *33*, 5298.
- (40) Hall, K. B.; McLaughlin, L. W. *Biochemistry* **1991**, *30*, 10606.

- (41) Breslauer, K. J.; Frank, R.; Blocker, H.; Marky, L. A. *Proc. Natl. Acad. Sci. U.S.A.* **1986**, *83*, 3746.
- (42) Xia, T.; SantaLucia, J.; Burkard, M. E.; Kierzek, R.; Schroeder, S.; Jiao, X.; Cox, C.; Turner, D. H. *Biochemistry* **1998**, *37*, 14719.
- (43) Sugimoto, N.; Nakano, S.; Katoh, M.; Matsumura, A.; Nakamuta, H.; Ohmichi, T.; Yoneyama, M.; Sasaki, M. *Biochemistry* **1995**, *34*, 11211.
- (44) SantaLucia, J., Jr. *Proc. Natl. Acad. Sci. U.S.A.* **1998**, *95*, 1460.
- (45) Holbrook, J. A.; Capp, M. W.; Saecker, R. M.; Record, M. T., Jr. *Biochemistry* **1999**, *38*, 8409.
- (46) Chalikian, T. V.; Volker, J.; Plum, G. E.; Breslauer, K. J. *Proc. Natl. Acad. Sci. U.S.A.* **1999**, *96*, 7853.
- (47) Marky, L. A.; Rentzeperis, D.; Luneva, N. P.; Cosman, M.; Geacintov, N. E.; Kupke, D. W. *J. Am. Chem. Soc.* **1996**, *118*, 3804.
- (48) Kankia, B. I.; Uedaira, H.; Ishimura, M.; Buckin, V. A. Submitted to *J. Am. Chem. Soc.*
- (49) Krakauer, H. *Biopolymers* **1972**, *11*, 811.
- (50) Solie, T. N.; Schellman, J. A. *J. Mol. Biol.* **1968**, *33*, 61.
- (51) Manning, G. *Rev. Biophys.* **1978**, *11*, 179.
- (52) Pezzano, H.; Podo, F. *Chem. Rev.* **1980**, *80*, 365.
- (53) Granot, J.; Feigon, J.; Kearns, D. R. *Biopolymers* **1982**, *21*, 181.
- (54) Kankia, B. I.; Funck, T.; Uedaira, H.; Buckin, V. A. *J. Solution Chem.* **1997**, *26*, 877.
- (55) Kankia, B. I.; Funck, T.; Marky, L. A. *J. Solution Chem.*, in press.
- (56) Millero, F. J.; Ward, G. K.; Lepple, F. K.; Hoff, E. V. *J. Phys. Chem.* **1974**, *78*, 1636.
- (57) Skerjanc, J.; Strauss, U. P. *J. Am. Chem. Soc.* **1968**, *90*, 3081.
- (58) Lown, D. A.; Thirsk, H. R.; Lord Wynne-Jones. *Trans. Faraday Soc.* **1968**, *64*, 2073.
- (59) Buckin, V. A. *Biophys. Chem.* **1988**, *29*, 283.
- (60) Marky, L. A.; Kupke, D. W. *Methods Enzymol.*, in press.